# Selectable functionalization of single-walled carbon nanotubes resulting from $CH_n$ $(n=1-3)$ adsorption

Feng Li,[1,2] Yueyuan Xia,[1] Mingwen Zhao,[1] Xiangdong Liu,[1] Boda Huang,[3] Zhenyu Tan,[4] and Yanju Ji[1]
[1]*School of Physics and Microelectronics, Shandong University, Jinan, Shandong, 250100 China*
[2]*Department of Physics, Taishan University, Taian, Shandong, 271021 China*
[3]*School of Information Science and Engineering, Shandong University, Jinan Shandong, 250100 China*
[4]*School of Electrical Engineering, Shandong University, Jinan, Shandong, 250161 China*
(Received 13 November 2003; published 27 April 2004)

Chemical functionalization of single-walled carbon nanotubes with different hydrocarbon radicals through collisional reaction between energetic methane molecule and single-walled carbon nanotubes in the energy range from 5 to 100 eV has been studied by using classical molecular dynamics simulations combined with *ab initio* calculations. We find that through controlling the incident energy of the methane molecule, chemical decoration of single-walled carbon nanotubes with different hydrocarbon radicals $CH_n$ $(n=1-3)$ can be achieved. Various stable adsorption configurations and the corresponding electronic structures are studied based on *ab initio* calculations. It indicates that for the $CH_3$ and CH radicals decorated (5,5) single-walled carbon nanotube, the density of states of the electrons is substantially modified.

DOI: 10.1103/PhysRevB.69.165415 PACS number(s): 73.22.−f, 73.63.Fg, 82.30.Cf

## INTRODUCTION

The novel structure and properties of carbon nanotubes have attracted great attention in both the fundamental science and technological applications ever since their discovery in 1991.[1] Carbon nanotubes exhibit the highest Young's modulus and tensile strength among all materials, and are promising low-density high-modulus fibers for using as reinforcing elements in composite materials.[2–11] Single-walled carbon nanotubes (SWNT's) are always described by rolled graphene where hexagonal two-dimensional lattice is mapped on a cylinder of radius $R$ with various helicities characterized by a set of two integers $(m,n)$. Their electronic structure can be either metallic or semiconducting, depending on the helicity and the radius.[12] These diverse electronic properties open a possibility of developing nanoelectronic devices by combining metallic and semiconducting nanotubes.[13]

Recently, functionalization of SWNT's achieved through adsorption of foreign molecules or radicals on the sidewall of SWNT's (Refs. 14–19) has come into focus since it is a promising way to modify the chemical, physical, and electronic properties of the tubes. For example, the sidewall decoration of SWNT's by a polymer matrix decreases the stiffness of the tubule by an average value of about 15%.[14,15] The transition of electronic structures from metallic to semiconducting caused by the adsorption of hydrogen atoms on the exterior wall of SWNT's has also been predicted.[16,17] Fluorization of SWNT's can modify the electronic structures by adjusting the coverage and the adsorption structure.[18,19] The coupling between the SWNT's and the foreign molecules or radicals usually disturbs the uniformity of charge distribution of SWNT's and introduces some local states in the band gap of the tubes,[20,21] and the global properties of the complex is thereby modified. In the present work, we study the adsorption of methane radicals on the exterior wall of SWNT's to explore the possibility of functionalization or modification of the SWNT's.

There are two main approaches to decorate SWNT's. One is noncovalent attachment of molecules (physical adsorption), the other is covalent attachment of functional groups (chemical adsorption) to the sidewall of SWNT's. The physical adsorption of some gas molecules on the wall of SWNT's can significantly change the electronic transport properties of SWNT's. The sensitivity of electronic properties of SWNT's to certain gas species makes SWNT's interesting candidates as nanoscale chemical sensors.[22] Different from the physical adsorption of adsorbates on SWNT's, for which the weak van der Waals forces between the adsorbed molecules and the SWNT's are dominant interactions, covalent functionalization of SWNT's arises from covalent attachment of functional radicals, and thus is more stable. In some cases, covalent functionalization is an especially attractive target, as it can improve solubility and processability and allows the unique properties of SWNT's to be coupled to those of other materials.

In general, chemical attachment of functional groups on the sidewall of defect-free SWNT's is relatively difficult, due to the relative low reactivity of the exterior surface of SWNT's. Polyatomic ion bombardment as an effective method of chemical functionalization of SWNT's has draw much attention both experimental and theoretical.[23,24] The main purpose of the present work is to study the decoration of SWNT's via collision of energetic methane molecules with SWNT's by using classical molecular dynamics simulations (MDS) combined with *ab initio* calculations. We found that energetic methane molecules can be decomposed into hydrocarbon radicals ($CH_3$, $CH_2$, and CH) adsorbing on the exterior wall of SWNT's, and hydrogen atoms in the collision. The decoration of SWNT's with different hydrocarbon radicals ($CH_3$, $CH_2$, or CH) resulted from methane bombardment depends on the incident energy of the methane molecule. When the incident energy is in the range from 15 to 25 eV, the functionalization of (5,5) SWNT with $CH_3$ radical has the highest probability. While the $CH_2$-

 

functionalized (5,5) SWNT is mainly observed as the incident energy ranging from 25 to 40 eV. The functionalization of (5,5) SWNT's with CH mainly occurs in the incident energy ranging from 40 to 70 eV. The electron-density contours obtained from *ab initio* calculations clearly shows that the hydrocarbon radicals are chemically adsorbed on the wall of the SWNT's. The modification of the electron density of states (DOS) of the SWNT's caused by the covalent functionalization with different hydrocarbon radicals was also obtained by using density functional theory (DFT).

## SIMULATION METHODS

The molecular collision processes between the methane molecules and the sidewall of (5,5) SWNT's, the subsequent methane molecular decomposition and the detailed process of hydrocarbon radicals adsorbed on the exterior wall of the SWNT forming various decoration structures were simulated using the second-generation reactive empirical bond order potential (REBO) developed by Brenner.[25] The earlier version of REBO (Ref. 26) has been widely used to describe hydrocarbon systems including diamond, graphite, carbon nanotube, and fullerenes. The results obtained are in good agreement with those from experiments and *ab initio* calculations. The second-generation REBO includes improved analytic functions and extended parameters based on the earlier version, and thus results in more accurate results. In addition, the long-distance van der Waals forces between the methane molecule and the SWNT and among the methane molecules expressed in 6-12 Lennard-Jones forms were also taken into account in our simulations.

Initially, a (5,5) SWNT with each end capped by a hemisphere of $C_{60}$, which contains 210 carbon atoms was relaxed for 2 ps at 0.1 K using a Langevin molecular dynamics scheme (LMD) in order to obtain the equilibrium configuration. LMD combines the simulated annealing scheme with MD calculations and allows one to heat or cool the reaction products in a physically appealing manner.[27] The equilibrium configuration of the (5,5) SWNT obtained was then used in the following simulations. A methane molecule placed 15 Å away from the (5,5) SWNT moves toward a hexagon on the wall of the tube in the central part of the tube at the translational velocity determined by the incident energy selected. Twenty incident energies were selected in the range of 5–100 eV. At the each selected energy, we simulated 20 events with the collision points randomly selected on the hexagon of the (5,5) SWNT. The orientation of the methane molecule was also randomly selected for each impact event. Following each collision event the system was relaxed freely for 1ps before the next collision event to commence.

## RESULTS AND DISCUSSION

We have examined various configurations of the reaction products following the collisions events. Four typical cases are found, and given as follows. (1) The methane molecule is scattered off the sidewall of the SWNT and no decoration of the SWNT occurs, (2) The decomposition reaction of methane $CH_4 \rightarrow CH_3 + H$ occurs and the $CH_3$ radical is adsorbed on the sidewall of the SWNT or it is scattered off the tube. (3) The decomposition reaction of methane $CH_4 \rightarrow CH_2 + 2H$ takes place and the $CH_2$ is adsorbed on the sidewall of the SWNT or it is scattered off the tube. (4) The reaction $CH_4 \rightarrow CH + 3H$ occurs and the CH radical is adsorbed on the sidewall of the SWNT or it is scattered off. The probability of these cases as a function of incident energy is shown in Fig. 1(a).

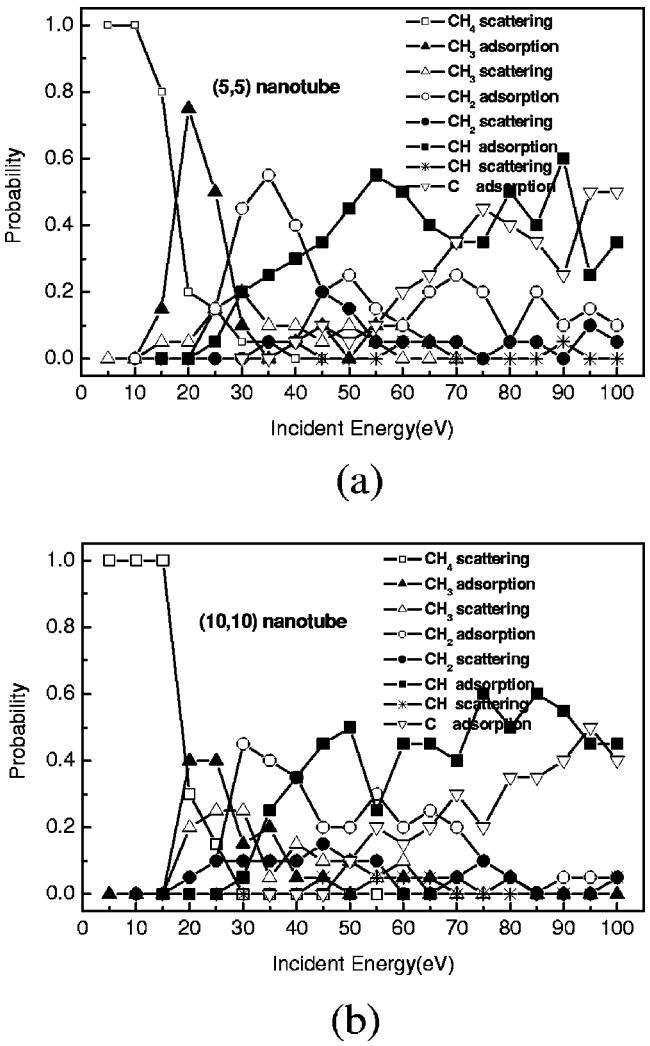


FIG. 1. Collisional reaction probabilities of various products and scatting events as a function of the incident energy of $CH_4$ molecule colliding with SWNT's, (a) $CH_4$ collision with a (5,5) SWNT, (b) $CH_4$ collision with a (10,10) SWNT.

It is obvious that the collision results strongly depend on the incident energy. When the incident energy is below 10 eV, 100% of the methane molecules are scattered, shown as the open squares in Fig. 1(a). When the incident energy is higher than 10 eV, the scattering probability for $CH_4$ decreases abruptly, with negligible probability at energy higher than 40 eV. As the incident energy is higher than 15 eV, decomposition reaction of methane $CH_4 \rightarrow CH_3 + H$ takes place. The sidewall decoration of the (5,5) SWNT with $CH_3$ radical has the maximum probability (the solid up triangles) at the incident energy of 20 eV, while the probability (the open up triangles) of $CH_3$ scattered off is always very low.

TABLE I. The selected bond lengths and adsorption energies of the (5,5) SWNT with different adsorbed hydrocarbon radicals. The adsorption energy $E_a$ of hydrocarbon radical ($CH_n$) on the sidewall of the SWNT is defined as the following expression: $E_a = E_{tot}(SWNT+CH_n) - E_{tot}(SWNT) - E_{tot}(CH_n)$, where $E_{tot}(SWNT+CH_n)$ is the total energy of SWNT with an adsorbed hydrocarbon radical, $E_{tot}(SWNT)$ and $E_{tot}(CH_n)$ are the total energy of an isolated SWNT and a free hydrocarbon radical, respectively. All the total energies are calculated based on fully relaxed configurations.

| | $d_{C_1\text{-}C_2}$ (Å) | $d_{C_1\text{-}C_3}$ (Å) | $d_{C_2\text{-}C_3}$ (Å) | $d_{C_1\text{-}H}$ (Å) | $E_a$ (eV) |
|---|---|---|---|---|---|
| $CH_3$-(5,5)SWNT | 1.542 | | 1.535 | 1.088 | −2.572 |
| $CH_2$-(5,5)SWNT(I) | 1.521 | 1.522 | | 1.113 | −4.563 |
| $CH_2$-(5,5)SWNT(II) | 1.653 | 1.653 | 1.640 | 1.079 | −3.895 |
| $CH_2$-(5,5)SWNT(III) | 1.521 | | 1.539 | 1.088 | −3.192 |
| CH-(5,5)SWNT(I) | 1.419 | 1.418 | | 1.089 | −4.721 |
| CH-(5,5)SWNT(II) | 1.657 | 1.656 | 1.645 | 1.080 | −2.978 |
| $CH_3$-(10,10)SWNT | 1.549 | | 1.527 | 1.089 | −2.238 |
| $CH_2$-(10,10)SWNT(I) | 1.520 | 1.520 | | 1.086 | −3.668 |
| $CH_2$-(10,10)SWNT(II) | 1.654 | 1.653 | 1.640 | 1.080 | −3.543 |
| $CH_2$-(10,10)SWNT(III) | 1.526 | | 1.533 | 1.090 | −2.855 |
| CH-(10,10)SWNT(I) | 1.395 | 1.395 | | 1.088 | −3.080 |
| CH-(10,10)SWNT(II) | 1.657 | 1.656 | 1.636 | 1.080 | −2.633 |

$CH_2$ radical appears when the incident energy is higher than 20 eV, and the adsorption probability (the open circles) of the $CH_2$ radical on the sidewall of the (5,5) SWNT has a maximum at the incident energy of 35 eV. The sidewall decoration of the (5,5) SWNT by adsorption of the CH radical mainly takes place at the incident energy higher than 30 eV, and the maximum probability of CH adsorption (the solid diamonds) appears at the incident energy of 55 eV. In addition to the three decoration structures described above, we have also found that when the incident energy is higher than 60 eV, the probability of complete dissociation of $CH_4$ molecule leaving behind the product carbon atom being adsorbed on the tube wall (the open down triangles) is relatively high.

It is also found that the collision of an energetic methane molecule with the SWNT can also lead to damage on the sidewall of the tube around the collision point, forming defects such as bond breaking, especially for the cases of high incident energy. However, most of these damages can be healed through annealing at higher temperature ($\sim$2000 K), provided the incident energy is lower than 70 eV. However, when the incident energy is higher than 70 eV, the severe damage formed and can not be healed simply through annealing.

The decomposition of methane molecule is relevant to the energy transfer from the translational energy to the internal energy caused by the collision. We have evaluated the energy required to detach a hydrogen atom from a methane molecule. The calculation based on REBO gives a value of 4.81 eV, in good agreement with that of 4.89 eV obtained from the GAUSSIAN98 code[28] at the accuracy level of B3LYP/6-31G*. When the incident energy is lower than 10 eV, the internal energy of a methane molecule gained in the collision is lower than 4 eV in all of our simulations. This is the reason why all the methane molecules scatter off the SWNT when the incident energy is lower than 10 eV. When the incident energy increases, methane molecule can obtain more internal energy and decomposition of $CH_4$ can take place, and thus adsorption of the produced radical on the tube wall can be observed since the radical is more active. We also notice that the decoration of the (5,5) SWNT with $CH_3$ radical has the highest probability ($\sim$75%) at incident energy 20 eV, which is about 10 eV higher than that reported for the collision between (5,5) SWNT and $CH_3$ radical.[23,24] This difference is understandable since extra energy is required to create a $CH_3$ radical through disintegration a hydrogen atom from a methane molecule.

We also simulated the collisions between an energetic methane molecule and a (10,10) SWNT under the same conditions used for the case of the (5,5) SWNT. The typical events found in these simulations are very similar to those found in the collision between methane molecule and the (5,5) SWNT. However, the probability corresponding to each decoration event is lower than that in the case of (5,5) SWNT, as shown in Fig. 1(b). For example, the maximum probability of the sidewall decoration of the (10,10) SWNT with $CH_3$ radical is only 40%, much lower than that of (5,5) SWNT, 75%. This is due to the lower reactivity of the carbon atoms on the sidewall of the (10,10) SWNT in comparison with that on the (5,5) SWNT since the curvatures of these two SWNT's are diffrent.[21] This is also in consistent with the result that the adsorption energy of a $CH_3$ radical on the sidewall of the (10,10) SWNT is about 0.334 eV weaker than that of a $CH_3$ radical on the sidewall of the (5,5) SWNT (see Table I).

It is interesting to examine the possible adsorption structures of methane radicals on the exterior wall of the SWNT's. There is only one stable configuration for a $CH_3$ radical being adsorbed on the sidewall of the (5,5) SWNT. The $CH_3$ radical always locates above a carbon atom on the tube wall. The equilibrium configuration of this adsorption complex after being relaxed at 0.1 K for 2 ps using LMD is shown in Fig. 2 (a). The electron density contours, obtained

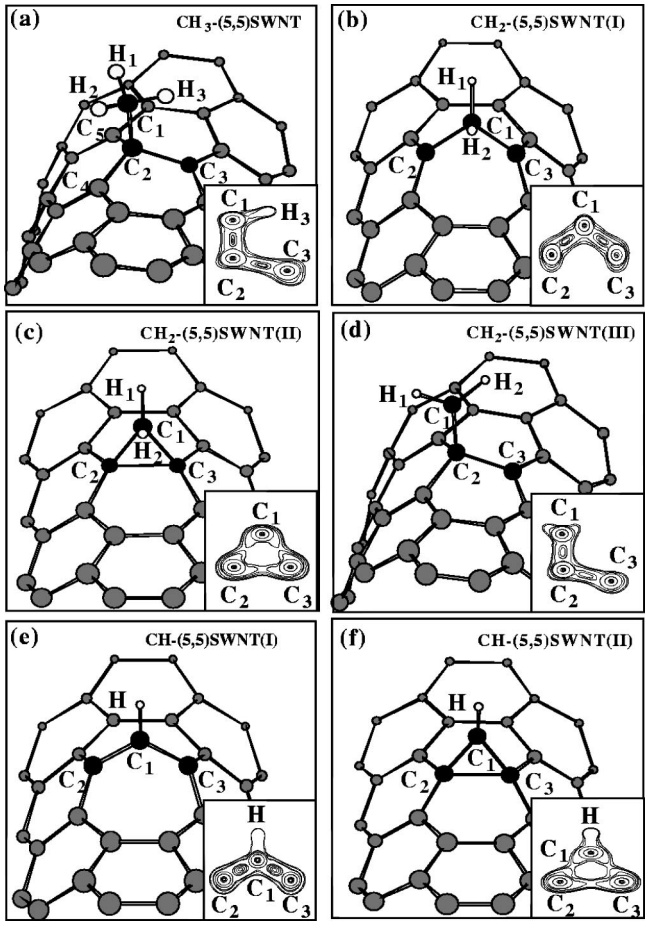


FIG. 2. The different decoration structures produced by $CH_4$ molecule collision with a (5,5) SWNT. The black ball ($C_1$) is the carbon atom of the $CH_n(n=1,2,3)$ radical and the black balls ($C_2$ and $C_3$) denote the carbon atoms at the adsorption sites on the SWNT, the gray balls denote carbon atoms on normally positions of the SWNT, and the small open balls represent hydrogen atoms. The insets of this figure are the electron density contours on the plane containing $C_1$, $C_2$, and $C_3$.

from DFT calculations, on the plane containing the carbon atoms $C_1$, $C_2$, and $C_3$ are also presented as the inset of this figure. The remarkable overlap of the electron clouds between carbon atoms $C_1$ and $C_2$ clearly indicates the formation of a covalent chemical bond between them. The length of this bond is about 1.542 Å, which is close to the length of covalent C-C bond in diamond. The adsorption energy of the $CH_3$ radical on the sidewall of (5,5) SWNT is $-2.57$ eV based on the calculation using REBO and $-2.44$ eV obtained from the computer code FIREBALL, which is base on density-functional theory tight-binding method (DFTB).[29] These results clearly show that the adsorption of a $CH_3$ radical on the sidewall of (5,5) SWNT is a chemical adsorption. Structural distortion also occurs in the region near the adsorption site caused by the adsorption of the $CH_3$, where the carbon atom $C_2$ extrudes out and the bond length between carbon atom $C_2$ and $C_3$ is lengthened to 1.535 Å in comparison with other C-C bonds on the tube wall, 1.42 Å. The bond angle between the bond $C_2$-$C_1$ and the bond $C_2$-$C_3$ is 110.1°, which is very close to the standard bond angles of $sp^3$ hybridization (109°), indicating structural transition of the carbon atoms around the adsorption site from $sp^2$ to $sp^3$ caused by the adsorption of the $CH_3$ radical.

We found three stable configurations for a $CH_2$ radical adsorbed on the sidewall of (5,5) SWNT. The first one is denoted by $CH_2$-(5,5)SWNT(I), as shown in Fig. 2(b). The carbon atom $C_1$ of the $CH_2$ radical bridges between the carbon atoms $C_2$ and $C_3$ of the tube, and the bond between $C_2$ and $C_3$ is broken. As shown in the inset of Fig. 2(b), the remarkable overlap of the electron clouds between $C_1$ and $C_2$, and that between $C_1$ and $C_3$ clearly indicates that the $CH_2$ radical is incorporated in the sidewall of the tube through two covalent bonds. The second one is denoted by $CH_2$-(5,5)SWNT(II), as shown in Fig. 2(c). In this case, the carbon atom $C_1$ bridges between carbon atoms $C_2$ and $C_3$ of the tubs, while the bond between $C_2$ and $C_3$ is not broken [see the inset of Fig. 2(c)]. The overlap of the electron cloud among carbon atoms $C_1$, $C_2$, and $C_3$ is somewhat loose in comparison with that of configuration $CH_2$-(5,5)SWNT(I). The distances between $C_1$ and $C_2$, $C_1$ and $C_3$, and $C_2$ and $C_3$ are 1.653, 1.653, and 1.640 Å, respectively. This indicates that $C_1$-$C_2$, $C_1$-$C_3$, and $C_2$-$C_3$ are still weak bonds. The third one is denoted by $CH_2$-(5,5)SWNT(III), as shown in Fig. 2(d). There, the $CH_2$ radical is adsorbed above a carbon atom $C_2$ on the tube through a covalent C-C bond with the bond length of 1.521 Å. We also evaluated the adsorption energies of $CH_2$ on the sidewall of the (5,5) SWNT corresponding to these three configurations based on REBO, respectively. The results are listed in Table I. $CH_2$-(5,5)SWNT(I) is energetically the most favorable configuration, while $CH_2$-(5,5)SWNT(III) is the most unfavorable. This is also revealed in our simulated annealing treatment. We relaxed the configuration $CH_2$-(5,5)SWNT(III) at 2000 K and found that it changed to the configuration $CH_2$-(5,5)SWNT(II) and then to the configuration $CH_2$-(5,5)SWNT(I). We also annealed the configurations $CH_2$-(5,5)SWNT(II) and $CH_2$-(5,5)SWNT(III) at 1000 K for 2 ps, but did not find any remarkable changes. We thus conclude that the configurations $CH_2$-(5,5)SWNT(II) and $CH_2$-(5,5)SWNT(III) are metastable, which may exist at room temperature.

The configurations of a CH radical adsorbed on the sidewall of (5,5) SWNT are relatively complicated. Four typical structures are observed and listed as following. (1) Carbon atom $C_1$ of the CH radical bridges between carbon atoms $C_2$ and $C_3$ of the tube forming two covalent bonds $C_1$-$C_2$ and $C_1$-$C_3$, while the bond $C_2$-$C_3$ originally existed on the tube wall is broken. This decoration structure is denoted by $CH_2$-(5,5)SWNT(I) in Fig. 2(e). (2) The carbon atom $C_1$ of the CH radical bridges between two carbon atoms $C_2$ and $C_3$ of the tube, but the bond between $C_2$ and $C_3$ is not broken, as denoted CH-(5,5)SWNT(II) shown in Fig. 2(f). (3) The carbon atom of the CH radical locates over the center of a hexagon on the tube wall with the distance about 1.646 Å to a carbon atom of the hexagon. We annealed this configuration at 1000 K for 2 ps using LMD, and did not found any remarkable change of the structure. However, as the annealing temperature increased to 2000 K, this configuration

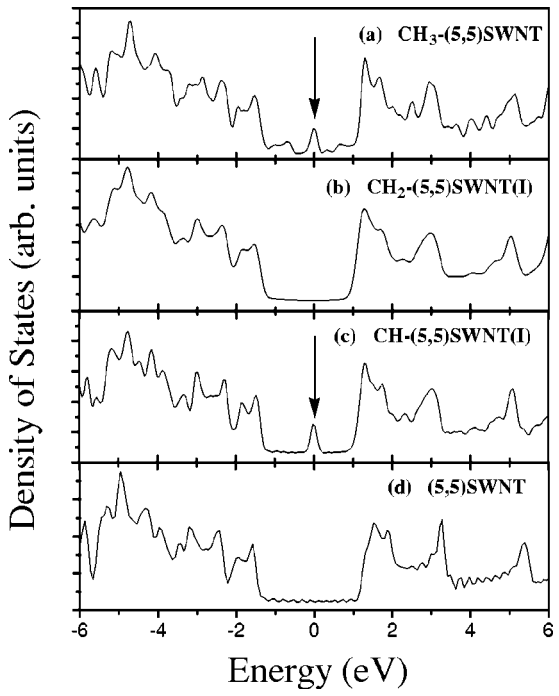


FIG. 3. Density of states (DOS) of electrons for different adsorption structures of $CH_n$ radicals adsorbed on (5,5) SWNT, (a) $CH_3$-(5,5)SWNT complex, (b) $CH_2$-(5,5)SWNT(I) complex, (c) CH-(5,5)SWNT(I) complex, and (d) a pure (5,5) SWNT.

changed to configuration CH-(5,5)SWNT(I), indicating that it is a metastable structure. (4) The CH radical substitutes a carbon atom of the tube wall, while the carbon atom is knocked out. The knocked out carbon atom is adsorbed on the interior wall of the tube or escapes from the other side of the tube. This structure mainly appears as the incident energy is in the range from 40 to 70 eV. The adsorption energies for these configurations clearly show that CH-(5,5)SWNT(I) is energetically most favorable (see Table I).

We also studied the DOS corresponding to the configurations $CH_3$-(5,5)SWNT, $CH_2$-(5,5)SWNT(I), CH-(5,5)SWNT(I), and a (5,5) SWNT without any decoration using DFT calculations.[29,30] It is obvious that the adsorption of a $CH_3$ or a CH on the sidewall of (5,5) SWNT modifies substantially the electron structure of the tube. Local states (denoted by the arrows) appear near the Fermi level of the tube as shown in Figs. 3(a) and 3(c). These local states are very important, since they facilitate the electron transport from occupied states to unoccupied states, and the electronic and the related optoelectronic properties of the decorated SWNT's can be thereby modified. It means that by adjusting the incident energy of the incident methane molecules and controlling the coverage of the adsorbed species, SWNT's can be functionalized, similar to the cases of hydrogen and fluorine atoms adsorbed on SWNT's.[16–19] However, when a $CH_2$ radical is adsorbed on the sidewall of (5,5) SWNT forming $CH_2$-(5,5)SWNT(I) complex, no local state appears around the Fermi level, as shown in Fig. 3(b). In this case the DOS near the Fermi level is very similar to that of a perfect (5,5) SWNT shown in Fig. 3(d). The analysis of the projected density of states (PDOS) of these functionalized tubs shows that for the $CH_3$-(5,5)SWNT complex the local state appearing near the Fermi level mainly results from the local carbon atoms $C_3$, $C_4$, and $C_5$ but not from the carbon atom $C_2$. The $sp^2$ to $sp^3$ transition of carbon atom $C_2$ causes $\pi$ bonds breakage near the adsorption site resulting in the local atoms $C_3$, $C_4$, and $C_5$ to contribute to the local state near the Fermi level. For the CH-(5,5)SWNT(I) complex, the local state observed near the Fermi level is caused by the atom $C_1$, since it has a dangling bond. This dangling bond results in substantial charge transfer around the adsorption site, which is found by Mulliken population analysis. However for the $CH_2$-(5,5)SWNT(I) complex, the PDOS of both carbon atom $C_2$ and $C_3$ are very similar to that of the other carbon atoms of the tube, indicating that the adsorption of $CH_2$ does not break the $\pi$ bonds on the tube wall. The localized carbon atom $C_1$ of $CH_2$ radical, which has the character of $sp^3$ hybridization, has a local state about 6.0 eV below the Fermi level. The local state is submerged in other states. Therefore, it is understandable that no local state appears near the Fermi level of $CH_2$-(5,5)SWNT(I) complex, since there is neither breaking of $\pi$ bonds nor dangling bond.

In summary, we studied the collisions of an energetic methane molecule with SWNT's for the incident energy ranging from 5 to 100 eV. We found that chemical functionalization of SWNT's with hydrocarbon radicals $CH_n$ ($n=1-3$) could be achieved through the collisions. The dependence of the functionalization of SWNT's on the incident energy suggests that SWNT's decorated by different hydrocarbon radicals ($CH_3$, $CH_2$, or CH) can be obtained by controlling the incident energy. The functionalization of (5,5) SWNT with $CH_3$ and CH changes the DOS of the tube near the Fermi level and may in turn modify its electronic and related optoelectronic properties.

## ACKNOWLEDGMENTS

This work is supported by the National Natural Science Foundation of China under Grant No. 10175038 and No. 10374059, the National Key Program of Fundamental Research under Grant No. G1999064502, and the Education Ministry of China under Grant No. 20020422012.

[1] S. Iijima, Nature (London) **354**, 56 (1991).
[2] M. M. J. Treacy, T. W. Ebbesen, and J. M. Gibson, Nature (London) **381**, 678 (1996).
[3] E. W. Wong, P. E. Sheehan, and C. M. Lieber, Science **277**, 1971 (1997).
[4] A. Krishnan, E. Dujardin, T. W. Ebbesen, P. N. Yianilos, and M. M. J. Treacy, Phys. Rev. B **58**, 14 013 (1998).
[5] P. Poncharal, Z. L. Wang, D. Ugarte, and W. A. de Heer, Science **283**, 1513 (1999).
[6] M-F. Yu, O. Lourie, M. J. Dyer, K. Moloni, T. F. Kelly, and R. S.

Ruoff, Science **287**, 637 (2000).
[7] J. M. Molina, S. S. Savinsky, and N. V. Khokhakov, J. Chem. Phys. **104**, 4652 (1996).
[8] M. Buongiorno Nardelli, B. I. Yakobson, and J. Bernholc, Phys. Rev. B **57**, R4277 (1998).
[9] T. Ozaki, Y. Iwasa, and T. Mitani, Phys. Rev. Lett. **84**, 1712 (2000).
[10] J. P. Lu, Phys. Rev. Lett. **79**, 1297 (1997).
[11] Y. Y. Xia, M. W. Zhao, Y. C. Ma, M. J. Ying, X. D. Liu, P. J. Liu, and L. M. Mei, Phys. Rev. B **65**, 155415 (2002).
[12] M. S. Dresselhaus, G. Dresselhaus, and P. C. Eklund, *Science of Fullerenes and Carbon Nanotubes* (Academic Press, San Diego, 1996).
[13] L. Chico, Vincent H. Crespi, Lorin X. Benedict, Steven G. Louie, and Marvin L. Cohen, Phys. Rev. Lett. **76**, 971 (1996).
[14] A. Garg and S. B. Sinnott, Chem. Phys. Lett. **295**, 273 (1998).
[15] Z. G. Mao, A. Garg, and S. B. Sinnott, Nanotechnology **10**, 273 (1999).
[16] O. Gölseren, T. Yildirim, and S. Ciraci, Phys. Rev. B **66**, 121401(R) (2002).
[17] K. S. Kim, D. J. Bae, J. R. Kim, K. A. Park, S. C. Lim, J. J. Kim, W. B. Choi, C. Y. Park, and Y. H. Kim, Adv. Mater. (Weinheim, Ger.) **14**, 1818 (2002).
[18] K. N. Kudin, H. F. Bettinger, and Gustavo E. Scuseria, Phys. Rev. B **63**, 045413 (2001).
[19] K. A. Park, Y. S. Choi, Y. H. Lee, and C. Kim, Phys. Rev. B **68**, 045429 (2003).
[20] M. W. Zhao, Y. Y. Xia, J. P. Lewis, and R. Q. Zhang, J. Appl. Phys. **94**, 2398 (2003).
[21] M. W. Zhao, Y. Y. Xia, Y. C. Ma, M. J. Ying, X. D. Liu, and L. M. Mei, Phys. Rev. B **66**, 155403 (2002).
[22] J. Kong, N. R. Franklin, C. W. Zhou, M. G. Chapline, S. Peng, K. Cho, and H. J. Dai, Science **287**, 622 (2000).
[23] B. Ni and S. B. Sinnott, Phys. Rev. B **61**, 16343 (2000).
[24] B. Ni, R. Andrews, D. Jacques, D. Qian, M. B. J. Wijesundara, Y. S. Choi, L. Hanley, and S. B. Sinnott, J. Phys. Chem. B **105**, 12719 (2001).
[25] D. W. Brenner, O. A. Shenderova, J. A. Harrison, S. J. Stuart, B. Ni, and S. B. Sinnott, J. Phys.: Condens. Matter **14**, 783 (2002).
[26] D. W. Brenner, Phys. Rev. B **42**, 9458 (1990).
[27] R. Biswas, and D. R. Hamann, Phys. Rev. B **34**, 895 (1986).
[28] M. J. Frisch, G. W. Trucks, H. B. Schlegeli, E. Scuseria, M. A. Robb, J. R. Cheeseman, V. G. Zakrzewski, J. A. Montgomery, Jr., R. E. Stratmann, J. C. Burant, S. Dapprich, J. M. Millam, A. D. Daniels, K. N. Kudin, M. C. Strain, O. Farkas, J. Tomasi, V. Barone, M. Cossi, R. Cammi, B. Mennucci, C. Pomelli, C. Adamo, S. Clifford, J. Ochterski, G. A. Petersson, P. Y. Ayala, Q. Cui, K. Morokuma, D. K. Malick, A. D. Rabuck, K. Raghavachari, J. B. Foresman, J. Cioslowski, J. V. Ortiz, B. B. Stefanov, G. Liu, A. Liashenko, P. Piskorz, I. Komaromi, R. Gomperts, R. L. Martin, D. J. Fox, T. Keith, M. A. Al-Laham, C. Y. Peng, A. Nanayakkara, C. Gonzalez, M. Challacombe, P. M. W. Gill, B. Johnson, W. Chen, M. W. Wong, J. L. Andres, C. Gonzalez, M. Head-Gordon, E. S. Replogle, and J. A. Pople, GAUSSIAN98, Revision A.6 (Gaussian, Inc., Pittsburgh, PA, 1998).
[29] O. F. Sankey and D. J. Niklewski, Phys. Rev. B **40**, 3979 (1989); J. P. Lewis, P. Ordejon, and O. F. Sankey, *ibid.* **55**, 6880 (1997); J. P. Lewis, T. D. Sewell, R. B. Evans, and G. A. Voth, J. Phys. Chem. **104**, 1009 (2000); J. P. Lewis, K. R. Glaesemann, G. A. Voth, J. Fritsch, A. A. Demkov, J. Ortega, and O. F. Sankey, Phys. Rev. B **64**, 195103 (2001).
[30] The supercells of perfect and decorated SWNT's selected in our calculations contain ten layers carbon atoms with periodical boundary condition along the tube axis, and 16 *k* points in Brillouin zone are included.